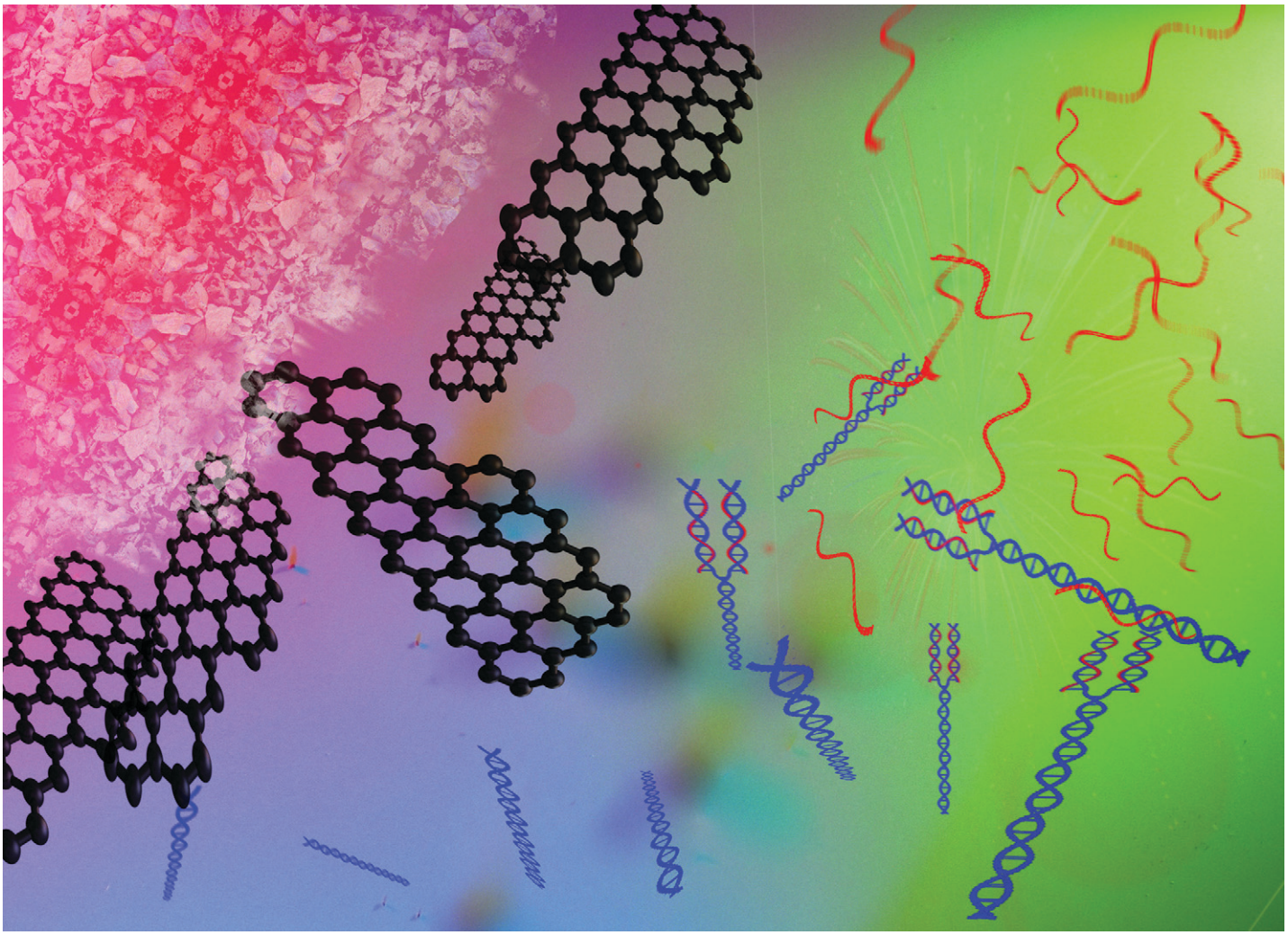

Featuring work from the Yager Lab at the University of Washington and PATH in Seattle, Washington, USA.

Title: Precision chemical heating for diagnostic devices

Electricity-free heaters are shown to be a viable alternative to conventional heating methods for isothermal nucleic acid amplification. A complete design strategy enables the design of precision chemical heaters for point of care use in low-resource settings.

As featured in:

See J. R. Buser *et al.*, *Lab Chip*, 2015, **15**, 4423.

ROYAL SOCIETY OF CHEMISTRY

www.rsc.org/loc

Registered charity number: 207890

Lab on a Chip

PAPER

View Article Online
View Journal | View Issue

Cite this: *Lab Chip*, 2015, **15**, 4423

Precision chemical heating for diagnostic devices†

J. R. Buser,‡*[a] S. Diesburg,‡[b] J. Singleton,[b] D. Guelig,[b] J. D. Bishop,[a] C. Zentner,[b] R. Burton,[b] P. LaBarre,[b] P. Yager[a] and B. H. Weigl[b]

Received 3rd September 2015,
Accepted 13th October 2015

DOI: 10.1039/c5lc01053e

www.rsc.org/loc

Decoupling nucleic acid amplification assays from infrastructure requirements such as grid electricity is critical for providing effective diagnosis and treatment at the point of care in low-resource settings. Here, we outline a complete strategy for the design of electricity-free precision heaters compatible with medical diagnostic applications requiring isothermal conditions, including nucleic acid amplification and lysis. Low-cost, highly energy dense components with better end-of-life disposal options than conventional batteries are proposed as an alternative to conventional heating methods to satisfy the unique needs of point of care use.

I. Introduction

Nucleic acid amplification tests (NAATs) have become essential tools for accurate, rapid diagnosis of infectious diseases.[1–3] This broad category of methods is, in many cases, replacing less sensitive protein-based tests for the differential diagnosis of symptomatic patients, as well as for surveillance in elimination efforts where the disease burden may be very low.

Despite their demonstrated utility, many NAAT technologies can only be used in laboratories with significant infrastructure and capital equipment and by users with extensive training. The required supplies, electrical power, and trained users are often unavailable in low-resource settings (LRS).[2,4] Decoupling NAAT diagnostics from these requirements could enable a new level of effective diagnosis and treatment at the point of care in LRS.[5–7]

Isothermal NAATs are potentially simpler alternatives to traditional NAATs because they do not require an energy-intensive precision thermal cycler.[8,9] These assays replicate target nucleic acid sequences at a single, constant temperature. To enable the use of isothermal NAATs in the lowest resource settings, PATH[10,11] and others[12–14] have demonstrated electricity-free approaches that employ exothermic chemical reactions coupled with a temperature-regulating phase change material (PCM) to process a sample at a precise temperature for an extended period of time. A useful phase change material must have an endothermic phase transition over a narrow temperature range centered at the temperature that one wishes to maintain. Devices using PCMs provide precision temperature control without requiring electricity, high levels of infrastructure, or large and expensive capital equipment. The development of such platforms is intended to meet the World Health Organization's recommended ASSURED guidelines for designing diagnostic tests that are affordable, sensitive, specific, user-friendly, rapid and robust, equipment-free, and deliverable to end-users.[15]

Effective electric, portable NAAT devices are becoming available with the commercialization of new, more compact PCR device platforms[3,16] such as the miniPCR mini8 (ref. 17) and Ahram Palm PCR.[18] These portable platforms could enable NAATs in LRS if electricity is available for recharging batteries. However, even where an electric grid exists in LRS, service is often intermittent,[19] and the intermittent supply of electricity for charging batteries may reduce productivity. Although the cost of these devices should continue to decrease, these devices are not appropriate for all LRS because of their reliance on grid electricity.

Although the ASSURED guidelines do not specifically require electricity-free solutions, there are settings in which advantages are apparent:

1. Where testing for extremely virulent pathogens (*e.g.*, Ebola virus[20]) and where immediate incineration or decontamination of entire devices may be desired.

2. Where electrical grid infrastructure is nonexistent or cannot support rechargeable battery-powered devices.

3. Where supply chain management fails to support instrument maintenance and consumable inventories, and a non-instrumented, integrated device is needed.

4. Natural disaster scenarios where large sections of the population are cut off from electricity sources for long periods.

5. When disposal of batteries or electronics is a concern.

[a] *Department of Bioengineering, University of Washington, Box 355061, Seattle, WA, USA. E-mail: buserj@uw.edu*
[b] *PATH: The Program for Appropriate Technology in Healthcare, Seattle, WA, USA*
† Electronic supplementary information (ESI) available. See DOI: 10.1039/c5lc01053e
‡ Contributed equally to this work.

Robust, electricity-free isothermal NAAT devices show great promise for expanding molecular diagnostic methods into LRS. However, challenges exist when designing devices to specific isothermal NAAT temperature requirements, and in accommodating their operation in uncontrolled ambient temperatures. As with electrical heating systems, system parameters can be adjusted to control the power source, temperature regulation, and integrated device performance. In this paper, we address these challenges and outline general design parameters.

Clearly, a point of care NAAT would ideally be small, fast, accurate, easy to use, and inexpensive—criteria that are often hard to meet at the same time. Under a grant from the Defense Advanced Research Projects Agency, a team including the University of Washington, PATH, the ELITechGroup, and the GE Global Research Center have collaborated to develop a platform for the application of chemical heaters to isothermal NAATs. The grant is entitled Multiplexable Autonomous Disposables for Nucleic Acid Amplification Tests for Limited-Resource settings (MAD NAAT).[21–26] One of the end-products of the project is a platform for an electricity-free, sample-to-result, point of care NAAT; the MAD NAAT platform takes a biological sample as input, prepares the sample by lysing the input cells using heat and enzymes, delivers the sample to a temperature-regulated zone for target nucleic acid sequence amplification, then delivers the amplicons to a lateral flow strip for readout. The precision heating requirements of the MAD NAAT project and the experience of the team with chemical heating applications have driven the development of the components, devices, and strategies presented in this paper.

Here, the requirements of the MAD NAAT device are used as the basis for discussion of:

1. General chemical heater design considerations.

2. Detailed design description of the chemical heater used in current MAD NAAT prototypes.

3. Experimental and computational results validating the MAD NAAT chemical heater as a stand-alone device, supporting an isothermal NAAT at varying ambient conditions.

We also highlight specific technical issues associated with implementation, and present an adaptable design process. That process combines engineering and finite element modeling, with the goal of enabling a design team working on similar problems to develop an optimized chemical heater.

II. General design considerations for chemical heaters

In the general design presented in this paper, a temperature-controlled chemical heater consists of an exothermic reaction thermally coupled with a temperature-regulating PCM, surrounded by insulation. Fig. 1 shows an exploded view of a generic chemical heater designed to incubate an isothermal NAAT.

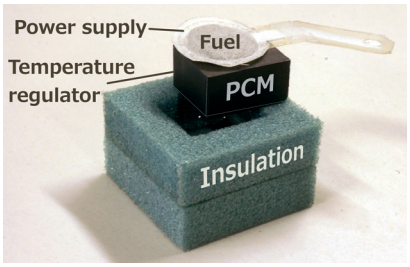

Fig. 1 Precision heater designed for use with isothermal NAATs, partially disassembled view. The diagnostic assay sits beneath the PCM block within an appropriate cut-out in the insulation. Top insulation omitted for clarity. A NaCl solution is delivered to this type of power supply *via* a paper wick from a reservoir (not shown).

II.A. Assay parameters

The design of a chemical heater is intrinsically tied to the assay for which it is designed, with critical assay parameters determining the fundamental heater specifications. The principal parameter is the optimal assay temperature, which defines the heater's nominal operating temperature. Another crucial parameter is the assay's tolerance to temperature fluctuation. Because biomolecular processes can have a narrow operating temperature range, relatively small temperature fluctuations can lead to large losses in assay sensitivity.

To achieve acceptable levels of sensitivity, the optimal temperature and associated tolerance should be quantified prior to design. This requires a series of experiments that vary the assay's temperature over a wide range. As an example, the MAD NAAT platform uses an isothermal strand displacement amplification[27,28] (iSDA, see ESI†), which is an isothermal NAAT with an operating temperature and tolerance of ~51 ± 4 °C. This level of precision temperature control is easily achievable with a benchtop thermal cycler (see ESI†). Variations in temperature can affect several aspects of assay performance, including efficiency and speed.

Two other assay parameters that are critical for defining heater specifications are (1) the maximum time it can take the sample to reach the operating temperature range (maximum warm up time) and (2) the minimum time the assay must be held in the operating temperature range (minimum holdover time). Both parameters should be defined relative to acceptable levels of overall assay sensitivity. Other important parameters that need to be considered include sample volume, sample format, size of the region to be heated, the range of environmental temperatures expected, and an acceptable volume for the entire heating system.

All of these parameters can have large implications regarding PCM choice, insulation requirements, device layout, and overall device size, as discussed in detail below. Assays which amplify effectively over a wide temperature range, experience the lowest possible susceptibility to performance loss as the system (sample and reagents) warms up to the operating temperature, and needs the shortest possible time for amplification are the simplest to design chemical heaters for. Fig. 2

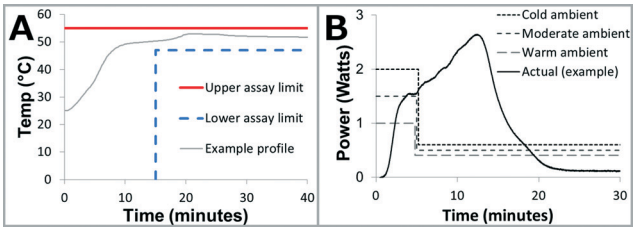

Fig. 2 Desired assay temperature tolerances and power curves. A: Assay temperature specifications. The minimum assay temperature here is 47 °C, and the temperature must warm up in 15 minutes or less, and hold for 25 minutes. To avoid permanently losing enzyme activity, this assay must never exceed 55 °C. An example temperature profile is shown (gray line) that meets these specifications. B: Ideal power profiles to achieve isothermal heating for a range of ambient temperatures, along with an example power profile from a chemical power supply. Cold ambient conditions need more power to warm the system up, in addition to needing more power to account for steady-state heat losses. The non-ideal power profile requires that temperature be additionally regulated by other means (*e.g.*, PCM).

shows the most important specifications related to temperature and time for a chemical heater given a specific assay.

II.B. Operating and environmental conditions

Although many diagnostic assays are currently used in temperature-controlled laboratories, fully realizing the advantages of testing at the point of care requires diagnostic devices that can accommodate a larger ambient temperature range. A design specification for ambient temperatures from 0 to 40 °C is not unreasonable for LRS. However, designing a device for a larger ambient temperature range means using a larger volume of insulation and PCM for a chemical heater.

Other environmental factors such as humidity levels, exposure to rain and wind, and shipping and storage conditions, can also affect the use of a chemical heater and should be considered at an early stage in the design process. Environmental factors can also dictate the need for either reusable or disposable designs. Table 1 shows the most basic information that should be known at the start of the design process, as well as the values specified for the MAD NAAT platform.

II.C. Chemical heater components

Chemical heaters that can meet the previously cited requirements typically need two main components: (1) a chemical power source and (2) a PCM temperature regulator. The power source provides heat at a predictable rate through an exothermic chemical reaction, and the PCM buffers the temperature by undergoing a phase change at a desired temperature.

The power source and temperature regulator combine to form the integrated system. Design elements can be categorized as either affecting the two components or the integrated system, as outlined in Table 2.

Power source. The foundation of the chemical power source is the exothermic reaction chemistry. The choice of chemistry dictates the thermal output and modes of control. Generally, the power source should use chemistry with high energy density, safe peak temperatures, nontoxic by-products, and reagents with minimal shipping and disposal restrictions. Table 3 shows examples of some commercial applications of exothermic reaction chemistries.

The design of a chemical heater is greatly influenced by the parameters of the power source. For chemistries with solid reactants, parameters such as particle size, packing density, chemical density, ratio of reactants, and reaction surface area will affect the thermal output. For chemistries with liquid reactants, parameters such as concentration and delivery rate will do the same. The geometry of the power source will also affect how the thermal output is delivered to the temperature regulator and sample, or is lost to the ambient environment.

Storage and activation of reactants influence the design of the integrated system. Reactants often have special storage requirements to maintain their integrity and must be kept separate prior to device operation. Because a controlled environment cannot be assumed in most LRS, storage needs should be understood and considered early in the design process. For example, water-reacting fuels must be kept from moisture, and iron–oxygen reactions must be prevented from contacting air during device manufacturing and storage.

Existing chemical heater design specifications can also affect the choice of chemistry. If a device is meant to be reusable, eutectic salts (*e.g.*, sodium acetate) may be a good fit.[29]

Table 1 Information needed for the design of a chemical heater for an assay application. These values are approximately those used for the MAD NAAT platform and are used for the example heater described in this paper

Assay temperature and tolerance	51 ± 4 °C
Ambient temperature range	15–30 °C
Maximum warm up time	15 minutes
Minimum holdover time	25 minutes
Assay liquid volume	40 μl in porous media
Heated zone form factor	Flat 2 × 2 cm
Reusability/disposability	Disposable

Table 2 Parameters used to achieve desired assay temperature and other device specifications

Power source
- Reaction chemistry, enthalpy of reaction, and reaction rate
- Particle size, packing density, and surface area of solid reactants
- Concentration of liquid/aqueous reactants
- Supply modality and supply rate of liquid reactants
- Geometry

Temperature regulator
- PCM phase change temp. range and latent heat capacity
- Thermal conductivity
- Geometry

Integrated system
- Containment of reactants and PCM
- Insulation
- Activation mechanism
- User interface

Table 3 Existing commercial products that use exothermic reactions for heat. Battery estimated energy capacities (estimated from manufacturer datasheets) are listed for comparison

Fuel	Reactants	Est. energy capacity	Sample consumer product
Calcium oxide	$CaO + H_2O$	1 kJ g^{-1}	Hot can[a]
Calcium chloride	$CaCl_2 + H_2O$	1 kJ g^{-1}	Rocket fuel coffee[b]
Iron filings	$Fe + 3O_2$	30 kJ g^{-1}	HotHands hand warmers[c]
Sodium acetate	$Na^+ + C_2H_3O_2$	0.3 kJ g^{-1}	Heat wave hand warmers[d]
Magnesium iron	$Mg–Fe + H_2O$	15 kJ g^{-1}	Field ration heaters for meals ready to eat (MREs)[e]
AA alkaline battery[f]	Zn/MnO_2	0.4 kJ g^{-1}	Remote control
Lithium coin cell CR2032[g]	Li/MnO_2	0.7 kJ g^{-1}	Laser pointer

[a] http://www.hot-can.com. [b] http://www.rocketfuel.uk.com. [c] http://www.hothandsdirect.com. [d] http://www.bentgrassconcepts.com. [e] http://www.luxfermagtech.com. [f] http://data.energizer.com/PDFs/E91.pdf. [g] http://data.energizer.com/PDFs/cr2032.pdf.

However, some user steps may be required to renew the power source. By contrast, if the entire device or just the fuel pack is considered a consumable and a high power density is needed, a water reaction such as the galvanic corrosion of a magnesium–iron blend with saline may be a good fit.

Other types of power sources are also possible. Sodium acetate solutions that have been supersaturated by cooling in the absence of nucleation sites are one example. The addition of a nucleation site causes exothermic crystallization of the salt. Although this power source may be desirable because it can be renewed by heating the sodium acetate solution (*e.g.*, the hand warmer application, see Table 3), it would require special design considerations. Example considerations include how nucleation will be triggered during the assay and how nucleation will be prevented during device construction, shipping, and storage.

The specific power source referenced in subsequent sections of this paper (including the detailed methods described in the ESI†) is the corrosion of mechanically alloyed particulate magnesium and iron (Mg–Fe) in the presence of saline. This Mg–Fe fuel and saline combination is a good fit for our application because it is easily stored, readily available, and inexpensive. It also allows for relatively straightforward activation mechanisms in an integrated chemical heater. Additionally, while electrical options are under consideration for powering MAD NAAT devices, Mg–Fe has a higher energy density than common inexpensive batteries (Table 3).

A model of the power source thermal output is necessary to accurately simulate the integrated device. This in turn enables more rapid system design iterations and optimization. A full system model describing the power output, chemistry, heat transfer, fluid dynamics, and phase change is, however, more complex than necessary to design a device. Instead, a power profile for chemical heaters is measured using a simple test fixture, and then used in modeling, as outlined below and in the ESI.†

Temperature regulator. The ideal source of heat for an isothermal assay would initially generate high power, to warm the sample from ambient to operating temperature, and then switch to low power to maintain the operating temperature in the face of inevitable heat losses to the environment (see idealized power profiles in Fig. 2B). However, design and manufacture of this power source as its own chemical heater would require some or all of the following:

- Adjustable power output based on varying ambient temperatures.
- Different reaction rates for the two power phases.
- Variable timing and actuation of multiple reactions.
- Active feedback controls.

A more practical design couples a single exothermic reaction with non-ideal power output (*e.g.*, any of the chemistries shown in Table 3) to a PCM temperature regulation component to restrict the sample temperature to the nominal operating temperature range.

The optimal assay temperature will dictate selection of the PCM on the basis of its melting (or boiling) temperature. For instance, if the assay temperature range is ~47 °C to ~55 °C, a PCM that changes phase at 51 °C has proven to be a good choice. The PCM must also have a narrow melting range that falls within the assay temperature range. The melting of a PCM can be monitored by many methods, including differential scanning calorimetry (DSC). Generally, on a plot of temperature *versus* heat input generated by DSC, a sharper-melting PCM is more effective at regulating temperature. Indeed, PCMs with similar peak melting temperatures may have different melting ranges,[30] in part because real materials have complex melting characteristics that depend on factors such as thermal history and chemical purity.

The thermal conductivity and latent heat capacity of the PCM are also critical to the design. A PCM with too little thermal conductivity will take too long to transfer heat from where it contacts the power source to the remote corners of its volume, resulting in increased warm up times and/or partial melting. Leaving a portion of the PCM unused for latent heat storage and release is wasteful. In practice, the thermal conductivities of many PCMs are too low for convenient chemical heater design – an issue that is addressed by incorporating additives with high thermal conductivity,[31–33] increasing the thermal conductivity of the resulting composite material. The use of aluminum wool and other shaped metals in PCM composites has been demonstrated.[34] However, in our experience it is difficult to produce void-free aluminum wool–PCM composites, resulting in inconsistent performance. The MAD NAAT device described in this paper

uses graphene nanoplatelet powder (N008-100-P-10, Angstron Materials, Dayton, OH, USA). In our experience, the graphene–PCM composites are easier to cast reproducibly and produce a larger range of thermal conductivities.

The minimum volume of PCM required with a particular power source depends on the ambient temperature range specification. In the optimal case and at the maximum ambient temperature, almost all of the PCM would melt and the sample would meet the maximum tolerable assay temperature for the minimum holdover time. In the optimal case and at the minimum ambient temperature, the sample would meet the minimum tolerable assay temperature within the maximum warm up time and for the minimum holdover time.

A large number of PCMs are readily available[35] from chemical suppliers. These range from specifically designed fatty acid composites from manufacturers such as Rubitherm, RGEES, or Entropy Solutions to organic compounds such as lauric acid or paraffin waxes.[36] Room temperature liquids such as water, acetone, and methanol can also serve as liquid-to-gas PCMs. If a PCM with the desired peak melt or boil temperature does not exist, PCMs can be combined to shift the peak melt temperature.[37] However, this can often have undesirable consequences, such as a wider or bimodal melt or boil range, lower latent heat, or both. Fortunately, there are many available PCM options in a range of melt temperatures that do not require additional engineering (Table 4).

The current version of the MAD NAAT chemical heater uses PureTemp 53 PCM (PT53, Entropy Solutions, Plymouth, MN, USA) to maintain the assay temperature within tolerance. As another example, a LAMP-based isothermal NAAT system developed at PATH operates at 63 °C.[10] At least two PCMs listed in Table 4 will provide that operating temperature. Additionally, a liquid-to-gas PCM is available because methanol boils near 63 °C (depending on elevation).

Integrated heater system. A successful design for an integrated system balances the need for thermal performance with practical considerations. These include sample introduction to and extraction from the heated zone, along with power source and PCM storage and activation. The primary design consideration for an integrated system is the spatial arrangement of the system components and insulation. The chemical power source and PCM regulator components must be coupled to the sample in a way that maintains adequate thermal transfer between the power source and the PCM regulator, and between the PCM regulator and the sample, while maintaining adequate thermal separation between the power source and the sample. Additionally, the integrated system must be insulated in such a way that the heater can provide adequate holdover time in the specified ambient temperature range.

The products of the power source chemical reaction also need to be considered. For example, the reaction of Mg–Fe with saline can rapidly reach the boiling point of the saline, and produces steam and hydrogen gas as by-products that need to be controlled. Proper handling of by-products is often required for safety, but other consequences of uncontrolled by-products, such as condensation in the sample zone, can also greatly affect thermal performance and device function.

At all stages of the design process, it is helpful to have working theoretical and finite-element thermal models of the integrated system (see ESI†). Such models enable effective iteration toward designs that provide adequate thermal performance in the least amount of space, among many other possible optimizations.

Table 4 Commercially available solid/liquid PCMs along with manufacturer specifications. Melt temperatures and latent heat values obtained from manufacturer websites[38–40] or from other published values[36,41]

Nominal melt temp [°C]	Name	Latent heat [J g^{-1}]
48	PureTemp 48	230
49	RT 50	168
49	Paraffin $C_{20–33}$	189
53	PureTemp 53	225
53	Myristic acid	181
55	RT 55	172
55	Stearic acid	159
58	PlusICE A58	132
58	PureTemp 58	225
60	PlusICE A60	145
60	RT 60	144
61	PureTemp 60	220
61	Palmitic acid	200
62	PlusICE A62	145
63	PureTemp 63	206
64	RT 64HC	230
65	RT 65	152
68	PureTemp 68	198

II.D. Deployment constraints

Additional design considerations can arise from deployment of the heater in a larger device. In some applications (*e.g.*, a heater for sample preparation), a heater should reach operating temperature as quickly as possible, whereas other applications may require a delay (*e.g.*, while waiting for an upstream process to complete). Two very different examples of successfully integrated chemical heater designs are (1) the NINA platform,[10,42,43] and (2) the MAD NAAT platform.[11,21,22,24] The NINA platform is optimized to provide incubation to assays in off-the shelf PCR tubes in a reusable vacuum thermos housing, but not integrated with other assay steps (*i.e.*, sample preparation, signal readout), whereas the MAD NAAT platform aims to integrate all assay steps and be disposable.

Many of the design considerations for the integrated chemical heater system apply to integration with a larger device. The specific arrangement of the chemical heater components within the larger device and with respect to the sample will continue to dominate thermal performance of the heater. The volume, geometry, and specific heat of other

media being heated within the larger device are also important considerations. A chemical heater expected to heat a sealed PCR tube[10] will be designed much differently than one designed to heat a postage stamp-sized section of porous membrane with inlet and outlet connections to other porous membranes.[11] The form of the heated zone will also affect the insulation requirements, heat capacity, form factor, and eventual cost of the larger device insulation and enclosure. Other heating requirements, such as boiling for lysis during sample preparation, will also affect thermal performance of the chemical heater.

Finally, the use case for the larger device must be defined. If a reusable device is desired, where many assays are to be performed under a single chemical heater, it may be useful to design for robust, repeatable performance using insulating housings like a vacuum thermos[10] or Styrofoam box.[14] Alternately, a device meant to be fully disposable will likely use less expensive and more disposable materials and have a smaller form factor.[11–13]

III. Detailed prototype components

Prototypes of the chemical power source and PCM thermal regulator components have been designed according to the previously outlined criteria. These prototype components are used in the integrated MAD NAAT device, in the stand-alone NINA amplification platform, and as a prototype integrated chemical heater system, discussed in further detail below. The prototype chemical power source is the reaction of mechanically alloyed Mg–Fe powder with saline, and the prototype PCM thermal regulator consists of a PureTemp 53/graphene composite that is solid at room temperature.

III.A. Power source

Many variables can affect the performance of chemical power sources. A non-exhaustive exploration of selected variables for the Mg–Fe/saline reaction is outlined below. In all experiments, except for the calorimetry experiments, the Mg–Fe fuel was contained in a heat-sealed pouch made of paper tea bag material. Glass fiber porous membranes were used as wicks to deliver and meter saline solution to the fuel packs. Additional details on the test setups and materials are found in the ESI† sections.

Particle size of solid reactants. Fig. 3A shows how fuel particle size influences the time needed for the temperature inside a custom calorimetry device to reach 90% of the maximum observed. Smaller particles have a larger relative surface area for a given mass of Mg–Fe, allowing the reaction to proceed more vigorously. Consequently, more energy is released earlier in the reaction, resulting in faster warm up times.

Shorter warm up times may be desirable for many applications, but the trade-off is that fuel will be exhausted sooner, resulting in less energy being released during later stages of the heating process. This condition may require additional PCM to adequately buffer the temperature, storing energy early to keep the sample warm later. Balancing these factors is important for system optimization.

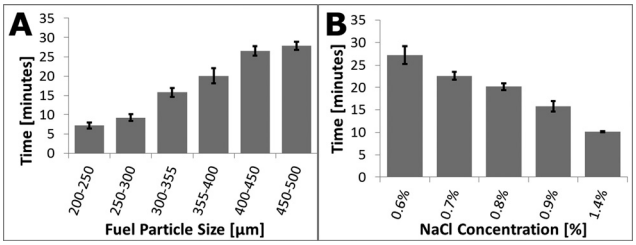

Fig. 3 A: Mean time to reach 90% of the peak reaction temperature for various particle sizes of Mg–Fe fuel, n = 6 minimum, error bars represent ± one standard deviation. B: Mean time to reach 90% of the peak reaction temperature is plotted for various saline concentrations. Reaction power output was quantified by monitoring temperature change in a lab-built calorimeter, n = 4 minimum, error bars represent ± one standard deviation.

Concentration of liquid reactants. Fig. 3B shows the warm up time for various saline concentrations. Increasing the concentration of NaCl resulted in shorter warm up times. Varying salinity over time may be desirable, but the trade-off is increased complexity of the saline delivery system. Nonetheless, this approach could decrease warm up time (high NaCl concentrations early) and extend holdover (low NaCl concentrations thereafter) with a slow, steady power output to match thermal loss to ambient surroundings and keep a stable operating temperature. Particulate NaCl can also be added to the fuel pack during assembly as a potential simplification of this approach. (Recent work from the University of Washington and PATH demonstrates a simple, ~95 °C chemical heater for bacterial sample preparation in which particulate NaCl is added to the fuel.)

Supply rate of liquid reactants. The volumetric flow rate of liquid reactant to the exothermic reaction also affects device warm up time. Delivering the liquid reactants through a wicking porous medium is a relatively simple means for continuously supplying the reaction with fluid. Conveniently, the principles of paper microfluidics[44] can be applied to chemical heater power supplies, metering the delivery of liquid reactants in the simplest case.[13] Lengthening or thinning the porous wick,[13] or making it from a less permeable material, restricts liquid delivery and affects the power profile. Recent advances in paper microfluidics[24] could also be used to automate delivery of a series of reactants at varying concentrations, which could be used to create a bolus energy release (device warm up), followed by a period of lower power (temperature maintenance).

Chemical power source geometry. Geometric variations of the power source can have a large effect on power output and overall device performance. In addition to the width, length, and material of the saline delivery wick, the shape and coverage of the fuel bed by the wick (for more effective delivery of liquid reactants) is an important geometric consideration. Fig. 4 shows a simple comparison of two scenarios of wick overlap in the fuel bed, in which partial overlap resulted in

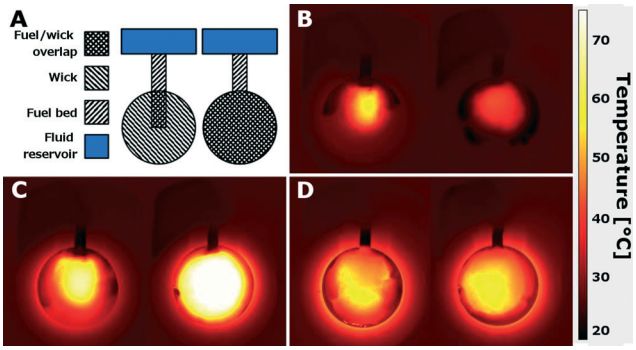

Fig. 4 Thermal images of fuel pack with varying wick coverage of the fuel bed. A: Top view schematic comparing fuel pack construction. The partial extension wick (left) extends only a short distance into the fuel, whereas the full profile wick (right) covers the entirety of the fuel bed. B: Temperature at 2 minutes into the reaction. Both fuel packs are at elevated temperature, but the partial wick is at higher temperature where the wick directly contacts the fuel bed. C: Temperature at 5 minutes. The partial wick has a more uneven temperature distribution, whereas the full profile wick is at a more uniform, higher temperature. D: Temperature at 20 minutes. The partial wick may have a more uneven temperature distribution than the full profile wick, but the difference is difficult to distinguish.

uneven temperature distribution in the fuel pack. Furthermore, the shape and size of the compartment or material confining the fuel pack (which expands during reaction) can also affect reaction rate based on compaction of the fuel and access to the liquid reactant.

Power source test fixture. A test fixture was constructed to characterize the chemical power source parameters such as fuel particle size and mass, saline volume, wick geometry, and fuel pack construction. The test fixture consists of an aluminum block, insulation, NaCl reservoir, and a cut-out for the chemical power source (see ESI† Fig. S1). The method of characterization was to determine the power output over time using the thermal characteristics of the test fixture (as determined with an electric heater). Temperature profiles measured within the test fixture were then converted to effective power profiles (efficiencies and losses due to non-ideal conductors and insulators are then taken into account by considering the effective power delivered as opposed to using total power output from the chemical reaction itself). Fig. 5 illustrates the impact on temperature and power of varying the length and width of the saline supply wick. The resulting power profiles can be reproduced in a computational model and used to predict integrated device performance (see ESI†) or simplified to step functions or average values and used in other, numerical calculations.

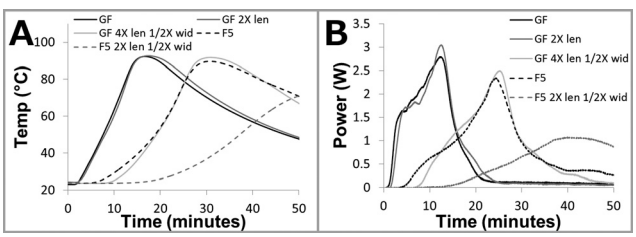

Fig. 5 Data from chemical power source characterization test fixture. A: Experimental time *vs.* temperature for various saline supply wick geometries. Power sources utilizing both glass fiber (GF) and Fusion 5 (F5) membranes can be tuned using membrane length and width. B: Profiles from panel A converted to time *vs.* power using the numeric model outlined in the ESI.†

III.B. Temperature regulator

For the MAD NAAT platform, the PCM temperature regulator was manufactured as a composite with graphene. As with the chemical power source, a PCM temperature regulator test fixture was constructed (see ESI†) to test the performance of graphene–PCM composites and to validate phase change models.

Mixtures with a higher percentage of graphene were higher in thermal conductivity (Fig. 6A). Although increased thermal conductivity is generally desirable, the trade-off is that a higher content of graphene in the mix means less PCM and less latent heat capacity (although recent work discusses the possibility of increased heat storage in certain materials due to graphene nanoparticle additives[33]). Increased graphene content decreased PCM latent heat capacity (Fig. 6B), resulting in decreased holdover time (Fig. 6C and D).

The manufacturing process developed for these prototype PCM temperature regulators (see ESI†) resulted in repeatable thermal conductivity measurements. However, a gradient, where thermal conductivity increased from bottom to top, was observed in casts. Shear mixing time, location along the

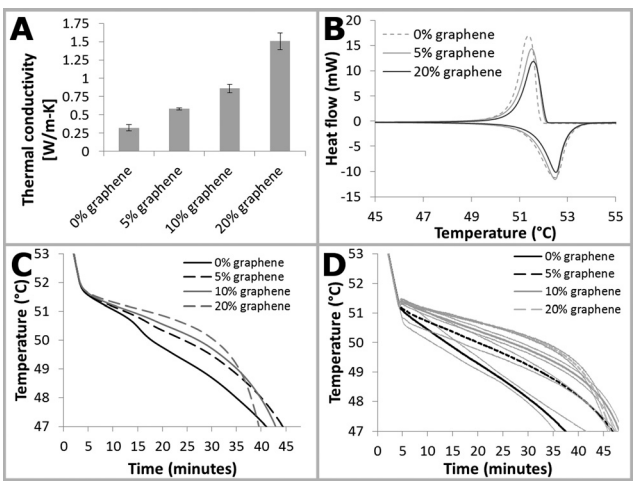

Fig. 6 Graphene effect on thermal properties. A: Thermal conductivity of various percentage graphene by weight in PureTemp 53 PCM. Thermal conductivity increases when graphene is added. Data is mean ± standard deviation, n = 6–8. B: DSC curves for graphene/PT53 PCM composites. Addition of graphene displaces PCM, resulting in a lower latent heat capacity of the composite (area under the curve in these plots). C: Modeled effect of varying graphene mass fraction. Lower graphene mass fractions have reduced holdover time. D: Experimental results for varying graphene mass fraction. A similar trend is observed as in the modeled results in panel C. Plotted is data mean ± one standard deviation, n = 2–3.

length of the casts, degassing by vacuum or other non-contact mixing means instead of tapping the mold, and the number of times the mold is tapped had little effect on conductivity.

Differences in graphene from the same manufacturer—such as differences in average platelet shape and grade—as well as in graphene from different manufacturers with similar nominal dimensions all affected the thermal conductivity of the PCM composite blocks. The batch-to-batch thermal conductivity coefficient of variation was approximately 3%, while the coefficient of variation due to machine error and test setup was about 0.1%.

Composite PCMs require adequate mixing to ensure the desired degree of homogeneity. Some protocols include degassing,[31] though this has not been necessary in our experience. The mixture is heated above the melting temperature while shear mixing to prevent solidification of the PCM. After mixing, the PCM composite should be cast in a manner that controls the solidification process. PCM shrinkage during cooling can produce voids in the casting, potentially impacting device reproducibility. In addition, crystallization can introduce heterogeneity into the final cast PCM composite.

One method to control solidification is to cool the bottom of the mold (*e.g.*, in a water bath) while heating the open top of the PCM. This allows a controlled solidification process, where the first portion to solidify is the lower portion of the casting. As the casting cools from the bottom up, the remaining liquid PCM on the top lowers as the solidifying PCM below shrinks, preventing voids from forming. This approach eliminates visible cavities and results in increased consistency (data not shown).

IV. Validation of the prototype integrated chemical heater system

After we constructed a prototype integrated chemical heater from the previously categorized components, the prototype heater performance was validated with an isothermal NAAT and against a finite element model of the system (see ESI†). Fig. 7 illustrates the design of the prototype integrated chemical heater, along with its thermal and assay performance.

IV.A. Prototype heater design and modeling

The following process was used to design the integrated chemical heater system:

1. Estimated the total fuel necessary for the assay.

2. Chose a chemical power source geometry and designed an appropriate fuel pack.

3. Produced fuel packs and reacted them in a chemical power source test fixture similar to the final device to tune the power output profile.

4. Chose a PCM and additive and designed the PCM temperature regulator.

5. Integrated the chemical power source with the PCM temperature regulator.

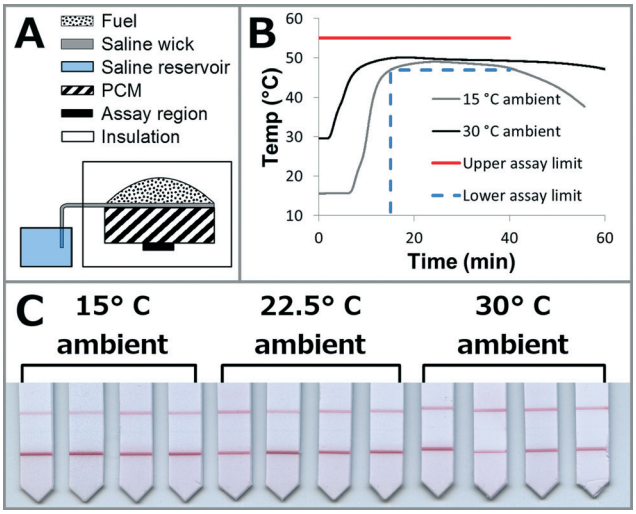

Fig. 7 Integrated chemical heater. A: Device schematic (not to scale). The fuel pack sits atop a PCM block, under which is the heated sample zone. A shell of insulation surrounds this assembly, with cut-outs for the fuel pack, PCM, and sample zone. B: Prototype thermal performance. The temperature measured in the assay region is plotted for 15 and 30 °C ambient temperatures. Plotted is the data mean, n = 3. The assay upper and lower limits are also plotted to visualize device temperature and time requirements. C: Lateral flow detection of iSDA nucleic acid amplification in a prototype device at 15, 22.5, and 30 °C ambient temperatures. Lower lines indicate presence of amplified product. Upper lines are biotin controls which bind the gold beads. Negative controls (not shown) indicate specificity of the reaction.

6. Modeled the initial design and materials using COMSOL with phase change, as discussed in the ESI,† for initial optimization of geometry for thermal transfer.

7. Completely built the initial design and tested it against performance targets (see Fig. 2A). We iterated until the heater reached the thermal design goals, including performance at various ambient temperatures.

IV.B. Prototype heater construction

For the prototype heater, placing the chemical power source above the PCM proved to be the most effective design (Fig. 7), with assay region contacting the bottom surface of the PCM thermal regulator. Saline is delivered from the reservoir to the fuel pack using a porous wick. The fuel is encapsulated as previously described. This power source sits atop a 2.6 × 2.0 × 1.2 cm PCM composite temperature regulator. The insulation consists of sections of polyvinyl chloride (PVC) foam with cut-outs for the fuel pack, wick, PCM, and assay region. The individual PVC foam components are held together by a double-sided adhesive. As the reaction proceeds, the fuel pack expands into a cut-out in the insulation lid. See ESI† for construction details.

IV.C. Prototype heater validation

The prototype heater held the sample within the assay tolerances for the required time (Fig. 7B). To confirm that this prototype heater could meet the thermal requirements of the

assay, iSDA amplification[27] (see ESI†) was performed within the heater across a range of ambient temperatures. The assay was performed in porous media because the prototype design was intended for integration with a paper microfluidic device. While the level temperature control achieved by the chemical heaters is not as precise as a benchtop thermal cycler (see ESI†), the temperature profiles in the sample region were sufficient to perform iSDA in ambient temperatures ranging from 15 °C to 30 °C, as evidenced by the assay results shown in Fig. 7C.

Conclusion

We have described a comprehensive approach and suite of tools that can be used to design chemical heaters for isothermal NAAT applications. Chemical heaters are especially appropriate where disposability or lack of electricity is a concern.

The use of test fixtures and models allows for evaluation of parameters such as fuel type, fuel particle size, reactant concentrations, fuel power output profile, PCM melt range, PCM thermal conductivity additives, and device geometry. These parameters then inform the design of an appropriate integrated chemical heater system.

If point-of-care diagnostics are to benefit from the use of precision chemical heaters for temperature control, additional studies will be needed regarding the stability of the magnesium iron fuel and phase change materials. Electric heaters are ubiquitous, and the electronics required for precision temperature control are readily available. Additionally, mass manufacturing, along with the quality control procedures needed to ensure reproducibility, are very well established for electronic components. In our hands, the magnesium iron fuel and PCM composites have been fairly robust and straightforward to work with. However, quality control procedures will be needed for the scaling up of manufacturing processes. The robustness of these devices in transport to low-resource settings and in storage remains to be studied.

Our future work includes continued use of these tools to further the development and integration of the MAD NAAT sample-to-result isothermal NAAT platform and additional exploration into new ways to control temperature, such as the use of liquid–gas transition PCMs. Subsequent advances in the use of phase change to control temperature could yield smaller devices, more precise control, and lessened requirements for device insulation.

Acknowledgements

Funding was primarily provided by DARPA DSO HR0011-11-2-0007 to Yager, the UW Department of Bioengineering, and PATH. Heater development at PATH was also partially provided by NIH (R01EB012641) and NIAID (R01AI097038). The iSDA assay reagents were provided by ELITechGroup Inc. Molecular Diagnostics as a part of the DARPA grant. We thank John Ballenot at PATH for the editorial support during manuscript preparation. We also thank everyone in the Yager and Lutz labs and collaborators at PATH, GE Global Research, and the ELITechGroup who provided support and feedback. The funders had no role in study design, data collection and analysis, decision to publish, or preparation of the manuscript.

Notes and references

1 M. A. Dineva, L. Mahilum-Tapay and H. Lee, *Analyst*, 2007, **132**, 1193.
2 UNITAID, *Tuberculosis: Diagnostic Technology Landscape*, World Health Organization, 2012.
3 A. Niemz, T. M. Ferguson and D. S. Boyle, *Trends Biotechnol.*, 2011, **29**, 240–250.
4 P. Yager, G. J. Domingo and J. Gerdes, *Annu. Rev. Biomed. Eng.*, 2008, **10**, 107–144.
5 B. H. Weigl, D. S. Boyle, T. de los Santos, R. B. Peck and M. S. Steele, *Expert Rev. Med. Devices*, 2009, **6**, 461–464.
6 P. K. Drain, E. P. Hyle, F. Noubary, K. A. Freedberg, D. Wilson, W. R. Bishai, W. Rodriguez and I. V. Bassett, *Lancet Infect. Dis.*, 2014, **14**, 239–249.
7 N. P. Pai, C. Vadnais, C. Denkinger, N. Engel and M. Pai, *PLoS Med.*, 2012, **9**, e1001306.
8 B. A. Rohrman and R. R. Richards-Kortum, *Lab Chip*, 2012, **12**, 3082–3088.
9 J. C. Linnes, A. Fan, N. M. Rodriguez, B. Lemieux, H. Kong and C. M. Klapperich, *RSC Adv.*, 2014, **4**, 42245–42251.
10 P. LaBarre, K. R. Hawkins, J. Gerlach, J. Wilmoth, A. Beddoe, J. Singleton, D. Boyle and B. Weigl, *PLoS One*, 2011, **6**, e19738.
11 J. Singleton, C. Zentner, J. Buser, P. Yager, P. LaBarre and B. H. Weigl, *Proc. SPIE*, 2013, **8615**, 86150R.
12 S. Huang, J. Do, M. Mahalanabis, A. Fan, L. Zhao, L. Jepeal, S. K. Singh and C. M. Klapperich, *PLoS One*, 2013, **8**, e60059.
13 C. Liu, M. G. Mauk, R. Hart, X. Qiu and H. H. Bau, *Lab Chip*, 2011, **11**, 2686–2692.
14 B. Hatano, T. Maki, T. Obara, H. Fukumoto, K. Hagisawa, Y. Matsushita, A. Okutani, B. Bazartseren, S. Inoue, T. Sata and H. Katano, *Jpn. J. Infect. Dis.*, 2010, **63**, 36–40.
15 D. Mabey, R. W. Peeling, A. Ustianowski and M. D. Perkins, *Nat. Rev. Microbiol.*, 2004, **2**, 231–240.
16 UNICEF, INNOVATIVE HIV POINT-OF-CARE (POC) CD4, *EID AND VIRAL LOAD EQUIPMENT PROJECT Early Infant Diagnosis (EID) and Viral Load (VL) POC TECHNOLOGY 2015*, 2015.
17 mini PCR|Science for Everyone, Everywhere, http://www.minipcr.com, accessed June 2015.
18 Ahram Biosystems Inc., http://www.ahrambio.com, accessed June 2015.
19 P. Yager, T. Edwards, E. Fu, K. Helton, K. Nelson, M. R. Tam and B. H. Weigl, *Nature*, 2006, **442**, 412–418.
20 J. J. Lowe, S. G. Gibbs, S. S. Schwedhelm, J. Nguyen and P. W. Smith, *Am. J. Infect. Control*, 2014, **42**, 1256–1257.
21 B. J. Toley, J. A. Wang, M. Gupta, J. R. Buser, L. K. Lafleur, B. R. Lutz, E. Fu and P. Yager, *Lab Chip*, 2015, **15**, 1432–1444.
22 N. Panpradist, B. J. Toley, X. Zhang, S. Byrnes, J. R. Buser, J. A. Englund and B. R. Lutz, *PLoS One*, 2014, **9**, e105786.

23 B. J. Toley, B. McKenzie, T. Liang, J. R. Buser, P. Yager and E. Fu, *Anal. Chem.*, 2013, **85**, 11545–11552.
24 S. Dharmaraja, L. Lafleur, S. Byrnes, P. Kauffman, J. Buser, B. Toley, E. Fu, P. Yager and B. Lutz, *Proc. SPIE*, 2013, **8615**, 86150X.
25 J. R. Buser, A. Wollen, E. K. Heiniger, S. Byrnes, P. C. Kauffman, P. D. Ladd and P. Yager, *Lab Chip*, 2015, **15**, 1994–1997.
26 S. A. Byrnes, J. D. Bishop, L. Lafleur, J. R. Buser, B. Lutz and P. Yager, *Lab Chip*, 2015, **15**, 2647–2659.
27 B. J. Toley, I. Covelli, Y. Belousov, S. Ramachandran, E. Kline, N. Scarr, N. Vermeulen, W. Mahoney, B. R. Lutz and P. Yager, *Analyst*, 2015, DOI: 10.1039/c5an01632k.
28 Y. S. Belousov, B. Alabeyev and N. Scarr, Methods for true isothermal strand displacement amplification, *US Pat Application*, US 14/202,637, 2014.
29 L. Lillis, D. Lehman, M. C. Singhal, J. Cantera, J. Singleton, P. Labarre, A. Toyama, O. Piepenburg, M. Parker, R. Wood, J. Overbaugh and D. S. Boyle, *PLoS One*, 2014, **9**, e108189.
30 J. Singleton, D. Guelig, J. Buser, R. Burton, O. Edeh, K. Hawkins, B. Weigl and P. LaBarre, in *IEEE Global Humanitarian Technology Conference (GHTC 2014)*, IEEE, 2014, pp. 721–725.
31 M. Mehrali, S. T. Latibari, M. Mehrali, H. S. C. Metselaar and M. Silakhori, *Energy Convers. Manage.*, 2013, **67**, 275–282.
32 F. Yavari, H. R. Fard, K. Pashayi, M. A. Rafiee, A. Zamiri, Z. Yu, R. Ozisik, T. Borca-Tasciuc and N. Koratkar, *J. Phys. Chem. C*, 2011, **115**, 8753–8758.
33 R. J. Warzoha and A. S. Fleischer, *Int. J. Heat Mass Transfer*, 2014, **79**, 314–323.
34 L. Fan and J. M. Khodadadi, *Renewable Sustainable Energy Rev.*, 2011, **15**, 24–46.
35 V. D. Bhatt, K. Gohil and A. Mishra, *Int. J. ChemTech Res.*, 2010, **2**, 1771–1779.
36 N. Ukrainczyk, S. Kurajica and J. Šipušiæ, *Chem. Biochem. Eng. Q.*, 2010, **24**, 129–137.
37 M. C. Costa, M. P. Rolemberg, L. A. D. Boros, M. A. Krähenbühl, M. G. de Oliveira and A. J. A. Meirelles, *J. Chem. Eng. Data*, 2007, **52**, 30–36.
38 PureTemp – Global Authority on Phase Change Material, http://www.puretemp.com, accessed July 2015.
39 RUBITHERM GmbH, http://rubitherm.de, accessed July 2015.
40 Phase Change Materials, PCM, *Thermal Management solutions*, http://www.pcmproducts.net, accessed July 2015.
41 A. Sarı, *Energy Convers. Manage.*, 2003, **44**, 2277–2287.
42 J. Singleton, J. L. Osborn, L. Lillis, K. Hawkins, D. Guelig, W. Price, R. Johns, K. Ebels, D. Boyle, B. Weigl and P. LaBarre, *PLoS One*, 2014, **9**, e113693.
43 R. Kubota, P. Labarre, J. Singleton, A. Beddoe, B. H. Weigl, A. M. Alvarez and D. M. Jenkins, *Biol. Eng. Trans.*, 2011, **4**, 69–80.
44 E. Fu, S. A. Ramsey, P. Kauffman, B. Lutz and P. Yager, *Microfluid. Nanofluid.*, 2011, **10**, 29–35.

